Modeling and Control of Doubly Fed Induction Generator Using Vector Control Method for Variable Wind Speed

Mozahid Hossain[1], Md. Alamgir Hossain[2*]

[1,2]Department of Electrical and Electronic Engineering, Khulna University of Engineering & Technology, Khulna-9203, Bangladesh
[*]Corresponding Author: mah@eee.kuet.ac.bd

ABSTRACT : In this paper Doubly Fed Induction Generator (DFIG) based wind turbine is investigated thoroughly to compensate for the variable voltage and transient introduced in the grid due to different wind speed. A reliable and robust vector control method is proposed for rotor side controller (RSC), grid side controller (GSC) for DFIG so that it can withstand with the grid in time of voltage dip that means it is capable of low voltage right through (LVRT) with the grid. By using state space representation and basic electrical equations of machines, the d-q model of the DFIG based wind turbine is presented this research. The performance of proposed method is explored considering active and reactive power controller, an MPPT, PI, and PID current controller. Additionally, a crowbar system is developed for over-current protection in time of voltage dip. For the performance comparison and validation of the proposed method, the system is simulated using MATLAB/Simulink environment.

KEYWORDS DFIG, rotor side controller, grid side controller, vector control, MPPT, LVRT.

I. INTRODUCTION

To cope with the worldwide electricity power demand, the power industries are continuously installing new wind power generation system. According to World Wind Energy Association, the wind power capacity hits the value of around 600 GW of which 53.9 GW added in 2018 and yearly growth is almost 24% [1]. Though wind power system is not particularly connected to weak power grid, due to the advancement of micro-grid, the integration of this power to isolated and weak grid network [2, 3] is increasing. Besides, this natural power system has pointed up the attention of the researchers to use it in offshore wind farm through high voltage direct current (HVDC) system. If wind power is not connected to grid, it must maintain the constant voltage and frequency instead of varying the rotor speed with wind speed and varying the loads. Hence, if the power produced being higher than demand, generation must be cut off controlling the blades' pitch angle. On the contrary, if it fails to produce sufficient power, load shedding method must be in action [4]. The increasing wind power results the increase of power penetration and impact on the utility grid. Therefore, wind turbine should have aerodynamic as well as power electronic converter based active power control [5, 6]. To meet these requirements, wind turbine should have the option of variable speed generation with pitch control and DFIG is the best option so far [7–9].DFIG in corporation with wind turbine is suitable for transferring wind energy to power grid.

DFIG is constructed by using wound rotor induction generator. It is a very special type of variable speed type generator. At present day, DFIGs are the foremost choice for wind power generation than any other generator topology because of its cost consideration since it uses a partial power converter instead of full power converter [10, 11].The generator has a distinctive reaction for the grid connectivity in which voltage source converter (VSC) can be used to control the rotor and the direct connection between stator and grid, the stator is directly affected by grid voltage fluctuations [10, 12]. To augment the tip-speed ratio of the turbine, the rotor is operated at variable speed within a defined controlled range of speed around the synchronous speed. The

generator has the option to operate in both sub-synchronous and super-synchronous speed. The speed of the rotor is controlled by 3-phase back-to-back VSC converter through slip ring that allow to handle approximately 30% of rated power. Figure 1 depicts the block diagram of DFIG based wind turbine power generation system.
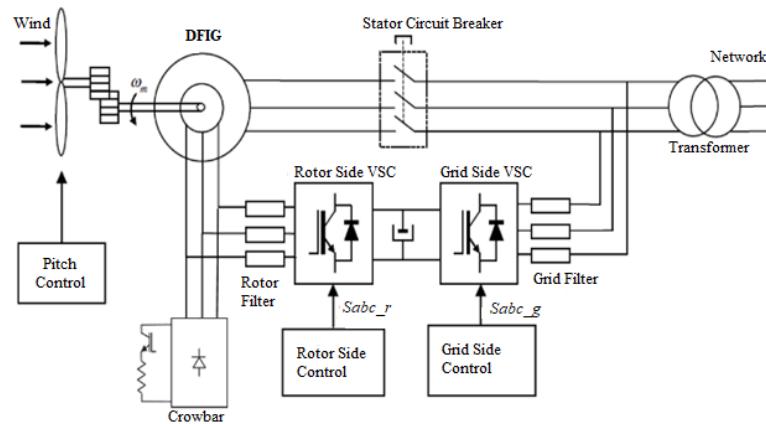

Figure 1: DFIG based grid connected wind turbine system

The different grid tie control system of the DFIG has been addressed in literature by the enthusiast researchers. In [13] authors have outlined a number of control systems for DFIG that includes a vast amount of references. However, the stand-alone operation of DFIG based wind turbines has not been explored much in the literature. An indirect stator-oriented vector control based on PI regulator is presented in [14] for providing constant voltage and frequency. But, PI controller is particularly applicable to compensate for the sate error from P controller and in terms of speed of the response and stability it depicts negative effect. To overcome these limitations, this paper suggests the vector control technique of DFIG using PID regulator for variable wind speed application and performance is compared with the use of PI regulator. A maximum power point tracking system is developed for RSC side. For overcurrent protection during voltage dip the crowbar system is introduced.

The paper is organized as follows. The dynamic modeling of DFIG and GSC are presented in Section II and Section III, respectively. In Section IV, the proposed vector-control scheme is obtained, and simulation results are discussed in Section V. Overall point of view is concluded in Section 6.

II.　DYNAMIC MODELING OF DFIG

With the help of space vector notation, the differential equations of the DFIG are modeled in *d-q* synchronous reference frame. The voltage space vectors of both stator and rotor side in synchronous reference frame can be represented by equations (1) and (2) respectively. The superscript '*a*' indicates that the space vectors are incorporated to a synchronous frame rotating at synchronous speed [15].

$$\bar{v}_s^a = R_s \bar{\imath}_s^a + \frac{d\bar{\psi}_s^a}{dt} + j\omega_s \bar{\psi}_s^a \tag{1}$$

$$\bar{v}_r^a = R_r \bar{\imath}_r^a + \frac{d\bar{\psi}_r^a}{dt} + j(\omega_s - \omega_m)\bar{\psi}_r^a \tag{2}$$

Where, the flux space vectors in the synchronous reference frame are given by the following equations (3) and (4). Note that, the superscript '*a*' has been eliminated from the space vectors in below expressions for simplicity.

$$\bar{\psi}_s = L_s \bar{\imath}_s + L_m \bar{\imath}_r \tag{3}$$

$$\bar{\psi}_r = L_m \bar{\imath}_s + L_r \bar{\imath}_r \tag{4}$$

The torque, stator and rotor side power expressions in *d-q* reference frame are given by the following equations,

$$P_s = \frac{3}{2}\text{Re}\{\bar{v}_s \bar{\imath}_s^*\} = \frac{3}{2}(v_{ds}i_{ds} + v_{qs}i_{qs}) \tag{5}$$

$$P_r = \frac{3}{2}\text{Re}\{\bar{v}_r \bar{\imath}_r^*\} = \frac{3}{2}(v_{dr}i_{dr} + v_{qr}i_{qr}) \tag{6}$$

$$Q_s = \frac{3}{2}\text{Im}\{\bar{v}_s \bar{\imath}_s^*\} = \frac{3}{2}(v_{qs}i_{ds} - v_{ds}i_{qs}) \tag{7}$$

$$Q_r = \frac{3}{2}\text{Im}\{\bar{v}_r \vec{\iota}_r\} = \frac{3}{2}\left(v_{qr}i_{dr} - v_{dr}i_{qr}\right) \tag{8}$$

$$T_{em} = \frac{3}{2}p\frac{k_r}{L_s'}\left[\psi_{rd}\psi_{sq} - \psi_{rq}\psi_{sd}\right] \tag{9}$$

Where, p expresses the number of pole pairs of the machine. The equation (10) represents the machine 'swing' equation that is composed by the electromagnetic torque T_{em}, the load torque, T_L comes from wind turbine, and the electrical angular speed of the rotor ω_m.

$$\frac{J}{p}\frac{d\omega_m}{dt} = T_{em} - T_L - b\frac{\omega_m}{p} \tag{10}$$

Where, J is the inertia in kg/m^2, comes from the combination of machine and turbine, and b is the speed dependent damping term.

Now, the following state-space representation in equation (11) of the DFIG is found by the expressions (1), (2), (3), (4), (9) and (10),

$$\begin{bmatrix} \frac{d\psi_{sd}}{dt} \\ \frac{d\psi_{sq}}{dt} \\ \frac{d\psi_{rd}}{dt} \\ \frac{d\psi_{rq}}{dt} \\ \frac{d\omega_m}{dt} \end{bmatrix} = \begin{bmatrix} -\frac{R_s}{L_s'} & \omega_s & k_r\frac{R_s}{L_s'} & 0 & 0 \\ -\omega_s & -\frac{R_s}{L_s'} & 0 & k_r\frac{R_r}{L_s'} & 0 \\ k_s\frac{R_r}{L_r'} & 0 & -\frac{R_r}{L_r'} & \omega_s-\omega_m & 0 \\ 0 & k_s\frac{R_r}{L_r'} & \omega_m-\omega_s & -\frac{R_r}{L_r'} & 0 \\ 0 & \frac{3}{2}\frac{p^2}{J}\frac{k_r}{L_s'}\psi_{rd} & 0 & -\frac{3}{2}\frac{p^2}{J}\frac{k_r}{L_s'}\psi_{sd} & -\frac{b}{J} \end{bmatrix} \begin{bmatrix} \psi_{sd} \\ \psi_{sq} \\ \psi_{rd} \\ \psi_{rq} \\ \omega_m \end{bmatrix} + \begin{bmatrix} 1 & 0 & 0 & 0 & 0 \\ 0 & 1 & 0 & 0 & 0 \\ 0 & 0 & 1 & 0 & 0 \\ 0 & 0 & 0 & 1 & 0 \\ 0 & 0 & 0 & 0 & -\frac{p}{J} \end{bmatrix} \begin{bmatrix} v_{sd} \\ v_{sq} \\ v_{rd} \\ v_{rq} \\ T_L \end{bmatrix} \tag{11}$$

Where,

$$k_s = \frac{L_m}{L_s}, \quad k_r = \frac{L_m}{L_r}, \quad L_s' = \sigma L_s, L_r' = \sigma L_r, \text{ and } \sigma = 1 - \frac{L_m^2}{L_r L_s} = 1 - k_s k_r$$

III. DYNAMIC MODELING OF GSC

The voltage space vector form of circuit between the GSC and the grid is given by

$$\bar{v}_f^a = R_f \vec{\iota}_g^a + L_f\frac{d\vec{\iota}_g^a}{dt} + \bar{v}_g^a + j\omega_a L_f \vec{\iota}_g^a \tag{12}$$

Where, $\bar{v}_f^a$ and $\bar{v}_g^a$ are voltage space vector at GSC side and the grid respectively. $\vec{\iota}_g^a$ is the grid side current, R_f and L_f are the grid side filter resistance and inductance respectively. So, the *d-q* components of the space vectors presented in equations (13) and (14) can be found by separating the space vectors into real and imaginary parts.

$$v_{df} = R_f i_{dg} + L_f\frac{di_{dg}}{dt} + v_{dg} - \omega_s L_f i_{qg} \tag{13}$$

$$v_{qf} = R_f i_{qg} + L_f\frac{di_{qg}}{dt} + \omega_s L_f i_{dg} \tag{14}$$

The whole active and reactive power exchanged through the GSC can be estimated by the following equations (15) and (16). In this paper, the voltage space vector $\bar{v}_g^a$ is aligned with the direct axis (d-axis) of the synchronously rotating frame. This assumption is most importantly required for the pursuit of vector control technique. Hence,

$$P_g = \frac{3}{2}v_{dg}i_{dg} = \frac{3}{2}|\bar{v}_g^a|i_{dg} = \frac{i_{dg}}{K_{Pg}} \tag{15}$$

$$Q_g = -\frac{3}{2}v_{dg}i_{dg} = -\frac{3}{2}|\bar{v}_g^a|i_{qg} = \frac{i_{qg}}{K_{Qg}} \tag{16}$$

IV. PROPOSED CONTROL STRATEGY

A vector control strategy is proposed for controlling the DFIG by using PID regulator. Figure 2 and 3 shows the proposed control block diagram of RSC and GSC respectively. Generally PI regulator is used for controlling the DFIG. By using PID regulator the performance of the DFIG is improved. With PID regulator,

the overall closed loop control system of rotor side control system can be represented by following equivalent second order system. Let, C(s) is the transfer function of PID regulator. So,

$$C(s) = k_p + s k_d + \frac{k_i}{s} \tag{17}$$

$$G'(s) = \frac{G(s)C(s)}{1 + G(s)C(s)} = \frac{\frac{k_d s^2 + s k_p + k_i}{\sigma L_r + R_r}}{s^2 + \frac{R_r + k_p}{\sigma L_r + k_d}s + \frac{k_i}{\sigma L_r + k_d}} \tag{18}$$

It can be found the value of k_p and k_i by $k_p = 2\xi\omega_n(\sigma L_r + k_d) - R_r$ and $k_i = (\sigma L_r + k_d)\omega_n^2$. Where, ξ is the damping constant and ω_n is the natural frequency of the system. Similarly it can be found the value of k_p and k_i for the grid side control system by following relations, $k_p = 2\xi\omega_n(L_f + k_d) - R_f$ and $k_i = (L_f + k_d)\omega_n^2$.

Rotor Current Reference Calculation:
The *d-q* rotor current references can be calculated by the electrodynamic torque of the machine and stator reactive power respectively. The *q* axis rotor current reference value is obtained by using electromagnetic torque $T_{em,}$

$$T_{em} = -\frac{3}{2}p\frac{L_m}{L_s}\left(\left(\psi_{sq}i_{dr} - \psi_{ds}i_{qr}\right)\right) \tag{19}$$

The flux space vector is aligned with *d*- axis. So, $\psi_{sq} = 0$ and $|\bar\psi_s| = \psi_{sd}$ here. Now the equation (19) becomes

$$T_{em} = -\frac{3}{2}p\frac{L_m}{L_s}\psi_{sd}i_{qr} = -\frac{3}{2}p\frac{L_m}{L_s}|\bar\psi_s|i_{qr} = k_T i_{qr}$$

$$\therefore i_{qr}^* = \frac{T_{em}^*}{k_T} \tag{20}$$

Equation (21) is used for calculating the *d*-axis rotor current reference by using the stator reactive power Q_s that is set by the operator or automatically when it is demanded in time of voltage dip that is normally kept to zero.

$$Q_s = \frac{3}{2}\left(v_{qs}i_{ds} - v_{ds}i_{qs}\right) = -\frac{3}{2}\omega_s\frac{L_m}{L_s}|\bar\psi_s|\left(i_{dr} - \frac{|\bar\psi_s|}{L_m}\right) = k_Q\left(i_{dr} - \frac{|\bar\psi_s|}{L_m}\right)$$

$$\therefore i_{dr}^* = \frac{Q_s^*}{k_Q} + \frac{|\bar\psi_s|}{L_m} \tag{21}$$

The stator flux amplitude $|\bar\psi_s|$ is constant and given by the following equation.

$$|\bar\psi_s| \cong \frac{|v_s|}{\omega_s} = \frac{\sqrt{\frac{2}{3}}V_s}{2\pi f_s} \tag{22}$$

Maximum Power Point Tracking (MPPT) System:
MPPT system is exploited to control the speed and to attain the maximum power from the wind speed. When, the wind turbine is trying to reach the maximum power point, the aerodynamic torque, T_t draw out by the wind turbine is given by the equation (23).

$$T_t = \frac{1}{2}\rho\pi R^3 \frac{R^2\Omega_t^2}{\lambda_{opt}^2}\frac{C_{p-max}}{\lambda_{opt}} = k_{opt-t}\Omega_t^2 \tag{23}$$

Where, $k_{opt-t} = \frac{1}{2}\rho\pi\frac{R^5}{\lambda_{opt}^3}C_{p-max}$, $\lambda_{opt} = \frac{R\Omega_t}{V_v}$, $C_p = C_{p-max}$, and $C_t = C_{t-opt}$. Including the damping term in equation (23) the electromagnetic torque, $T_{em} = -k_{opt}\Omega_m^2 + (D_t + D_m)\Omega_m$, where,

$$k_{opt} = \frac{1}{2}\rho\pi\frac{R^5}{\lambda_{opt}^3 N^3}C_{p-max} \tag{24}$$

Where, ρ denotes the air density, Ω_t denotes the angular speed of the rotor, *R* denotes the length of the blades (radius of the turbine rotor), *N* denotes the gear box ratio and V_v denotes the air velocity. $C_p(\lambda)$ denotes the coefficient of power and is frequently given as a function of the pitch angle (*β*) and the tip speed ratio (*λ*) defined by $C_p(\lambda) = k_1\left(\frac{k_2}{\lambda_i} - k_3\beta - k_4\beta^{k_5}k_6\right)\left(e^{k_7/\lambda_i}\right)$, where, $\lambda_i = \frac{1}{\lambda + k_8}$, $C_t(\lambda)$ denotes the torque coefficient given by $C_t(\lambda) = \frac{C_p(\lambda)}{\lambda}$.

Figure 4 shows the indirect speed controller (ISC) which tracks the maximum power corresponding to the wind speed available at the turbine blade. The high wind speed that can damage the WT without the MPPT system

flows through the turbine it takes an optimum power hence an optimum torque is also taken by the turbine given by the equation.
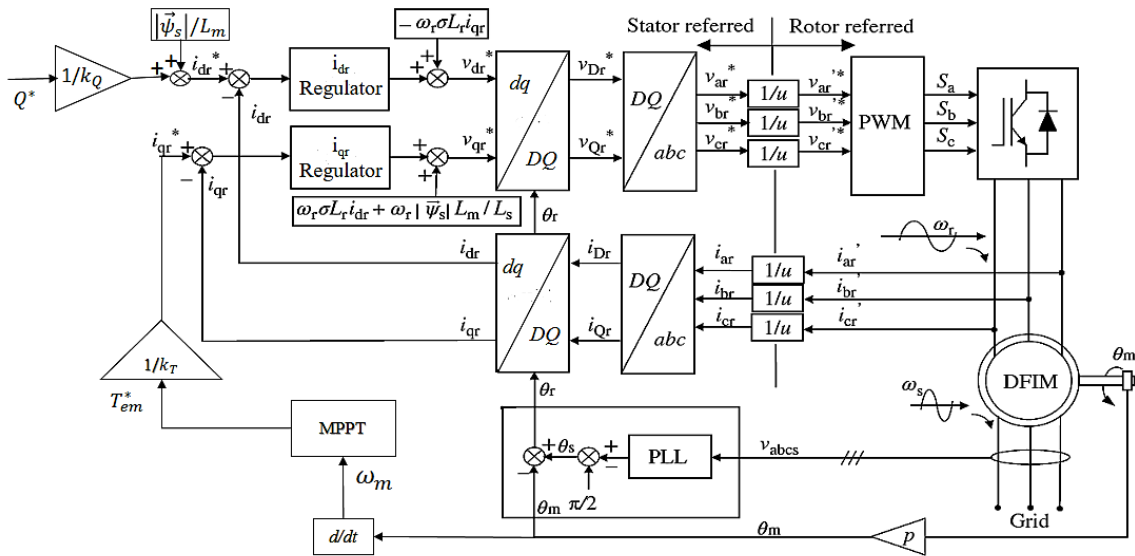

Figure 2: Vector control block diagram of rotor side converter of DFIG.
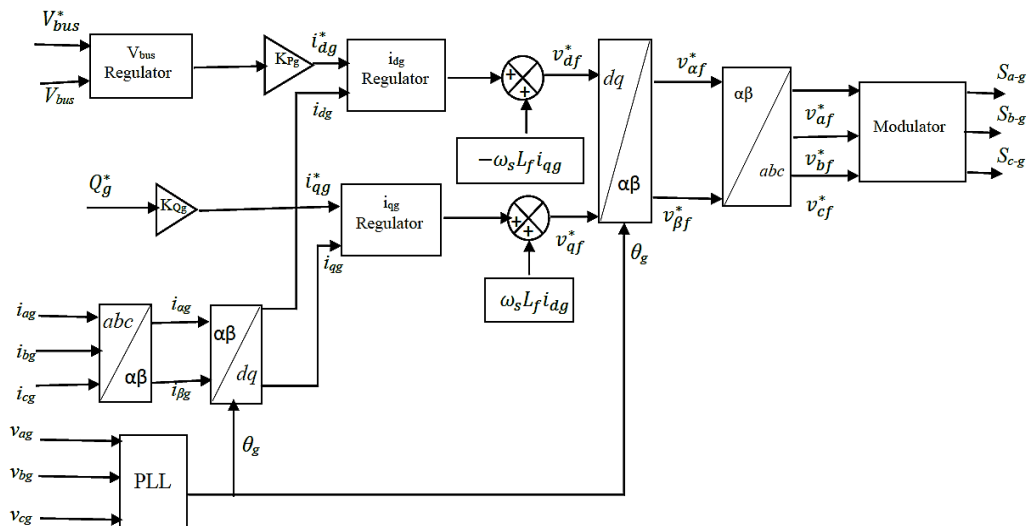
Figure 3: Block diagram of grid side converter.
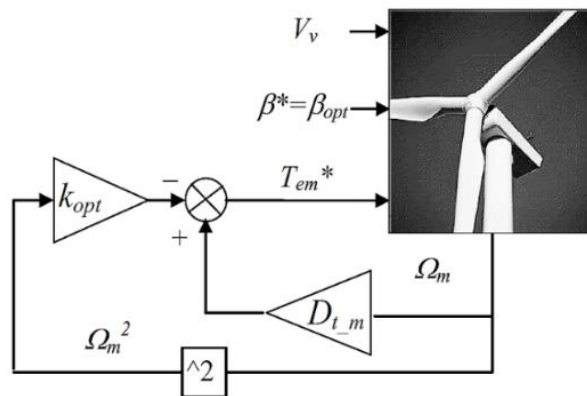
Figure 4: Indirect speed control (ISC).

V. SIMULATION RESULT AND DISCUSSION

In this section, the various characteristics of DFIG that is modeled in Simulink are inspected. The necessary simulation parameter are given in appendix. The Simulink model is created for a 2MW DFIG. The control strategy presented in this paper is vector control. Figure 5 shows the phase to neutral voltage waveforms of the stator side of the DFIG. For this generator, the phase to phase rms value of the voltage is set 690V. So, the phase to neutral voltage peak value will be 563.38V that is inspected from the waveforms of the Figure 5. The frequency the grid is 50Hz that is also found from the Figure 5 and 6.
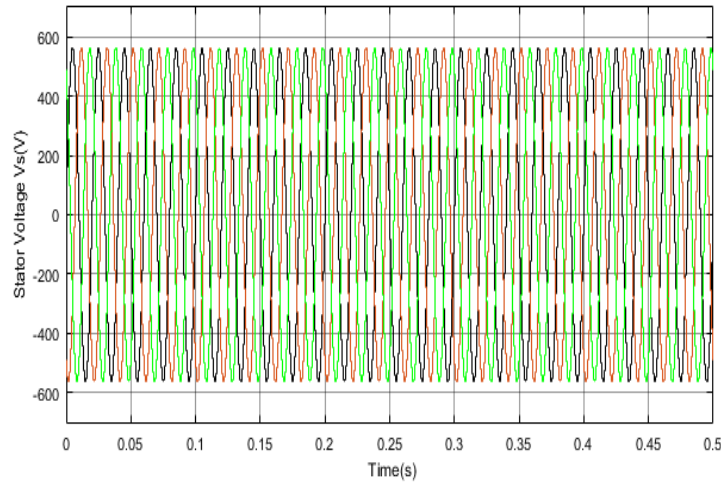
Figure 5: Stator side phase to neutral voltages
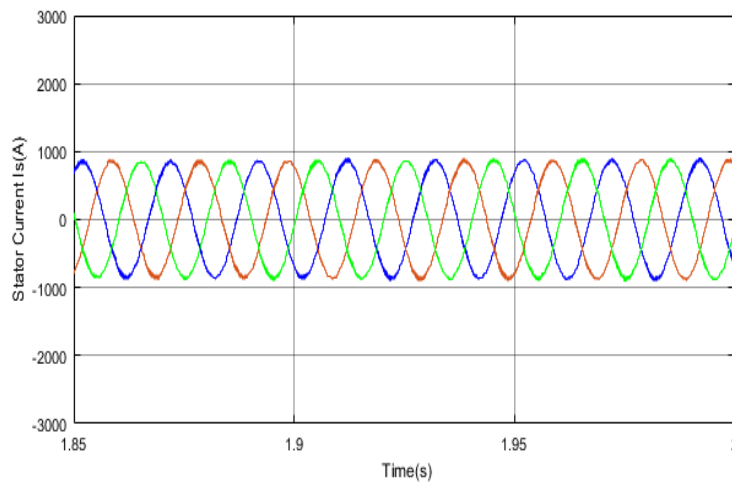
Figure 6: Stator side phase currents
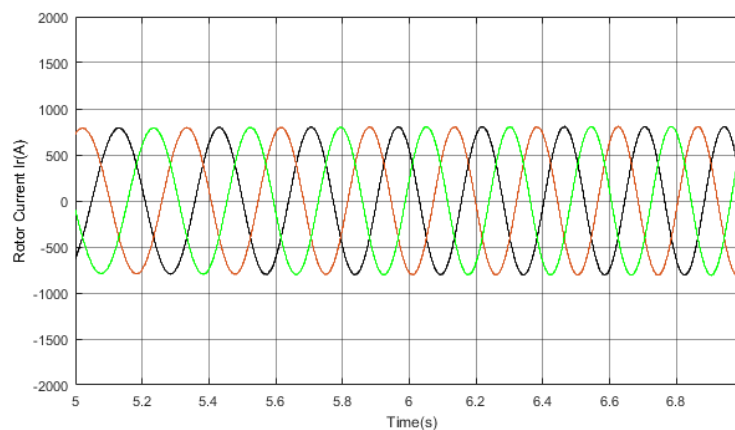
Figure 7: Rotor side phase current

Figure 6 shows the phase current waveforms of the stator side of the DFIG. From these two Figures it is seen that the voltage, currents and frequency are constant all the time under normal operating condition that is important to synchronize a generator with a grid system. Figure 7 shows the rotor side phase current waveforms. From this figure, it seen that the current amplitude is constant with time and also frequency. Here frequency of the current is different from stator side. The frequency of the rotor side current is found from slip frequency that is less than that of stator side. Figure 8 shows the DC link voltage V_{dc} which is constant at a value of 1150V. This voltage must be maintained at the constant value for proper operation of grid side and rotor converter. Power can be exchanged between RSC and GSC through the DC link. It is seen in Figure 8 that the voltage is very large at the starting of the generator and falls very quickly to its constant value.
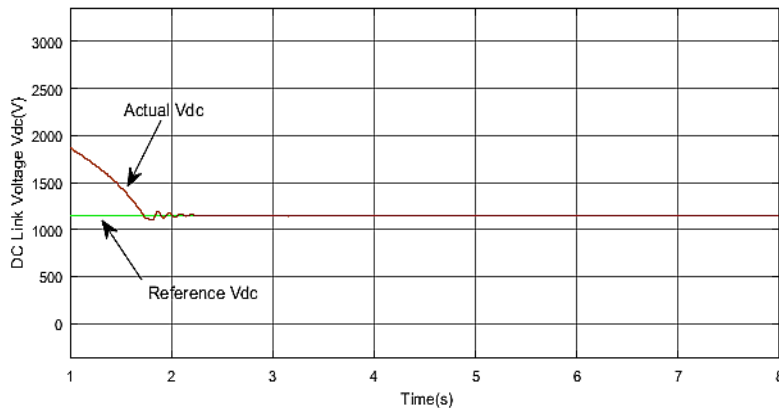
Figure 8: DC Link voltage

Figure 9 shows the output currents of grid side converter (GSC). It has some harmonics due to switching of the converter. The current is filtered by a filter called grid side filter. Its frequency is 50Hz and it must have the frequency of this value because it is connected to the 50Hz grid. Although it has some harmonics but it is very close to a sinusoidal wave. At the starting of the machine, there some overcurrent through the grid side filter due to initial overvoltage across the dc link capacitor as shown in Figure 9. But after some milliseconds the currents through grid filter become stable and sinusoidal in nature.
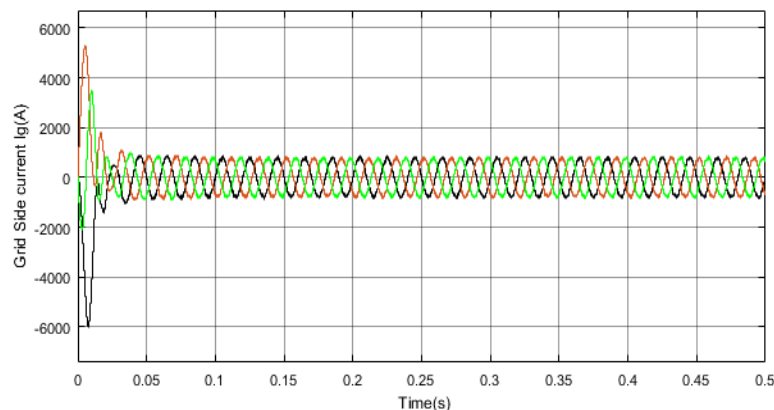

Figure 9: Grid side phase current waveforms I_{abcg}

The electromagnetic torque response of the machine is shown in Figure 10. The DFIG is modeled in motor reference frame, so the torque T_{em} is negative here for generator mode. From Figure 10, it is seen that firstly there is some difference in reference T_{em} generated by MPPT and after sometime the actual T_{em} follows accurately the reference T_{em}. It is seen that using PID the torque response is slightly distorted than PI, but the speed characteristics of the DFIG is improved that is shown in Figure 11(b) and reaches at steady state value more quickly. The speed is going up until it reaches at a constant speed that is about 170rad/sec for wind speed of 10ms^{-1}. The DFIG that is modeled in this work can operate variable wind speed for tracking maximum power. For each wind speed, there is a corresponding torque hence power to be extracted from wind.
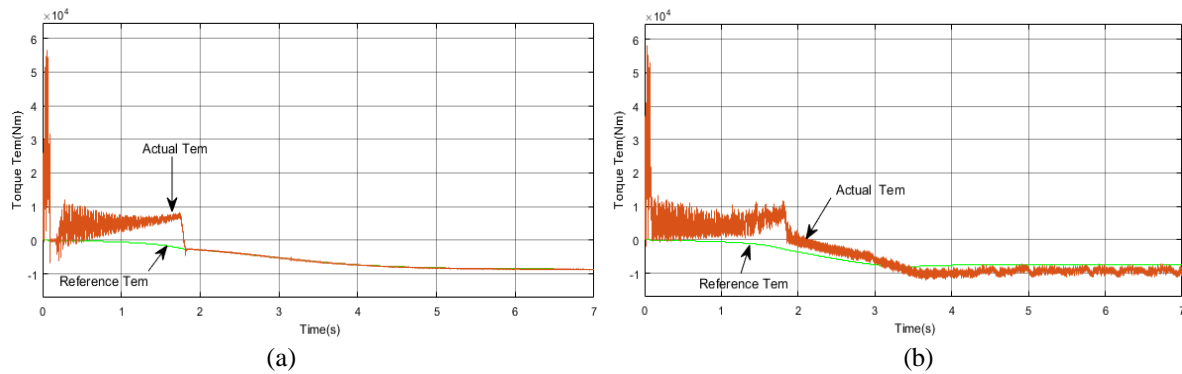
Figure 10: Torque response using (a) PI and (b) PID regulator
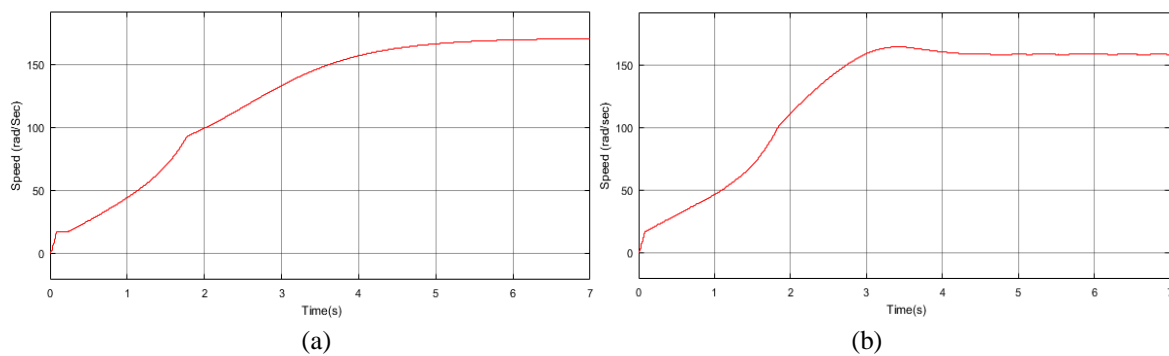
Figure 11: Speed of DFIG using (a) PI and (b) PID regulator

In the DFIG system, the power is injected to the grid both from rotor and stator side. Stator is directly connected to the grid and rotor is connected to the grid through RSC, DC link and GSC. About 30% of the total power is injected to the grid via RSC and GSC. Figure 12 shows the stator side active power curve at a wind speed of 10ms⁻¹ which is negative that indicates that power is injected to the grid because the DFIG is modeled in this work in motor convention for grid side active power curve the value will be positive.
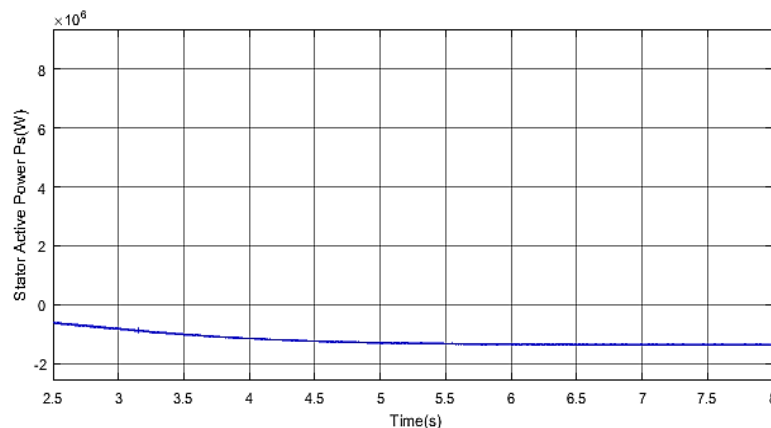
Figure 12: Stator side active power P_s

The total power at the grid injected by the generator should be maintained at a constant value. The fluctuation of power at PCC is prohibited. The total power P injected to the grid by the DFIG is the sum of grid side power P_g and stator side power P_s. Figure 13 shows the total power curve at grid that is supplied by the DFIG. The steady state power of DFIG is 1.5MW for wind speed10ms⁻¹ and 2.6MW for 12ms⁻¹ as seen in Figure 14. Also it is shown from these two Figures that there are some oscillations in the power curve at the starting of machine and after some few seconds the power becomes stable.
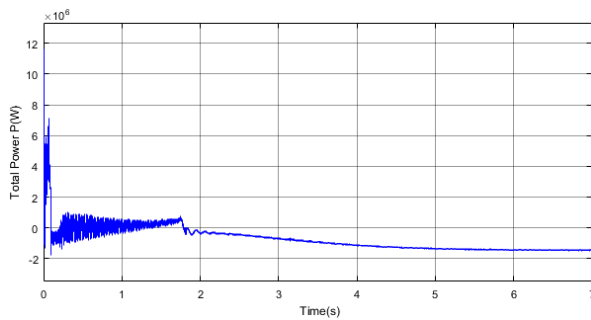
Figure 13: Total active power *P* at grid
at a wind speed of 10ms⁻¹
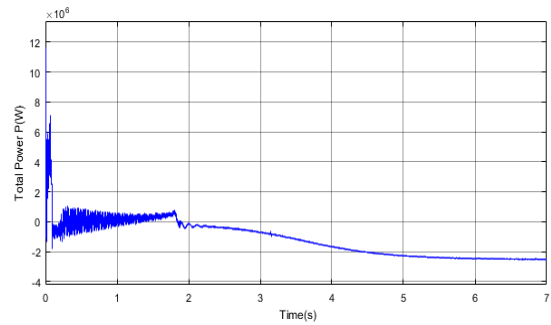
Figure 14: Total active power *P* at grid
at a wind speed of 12ms⁻¹

Normally the reactive power at grid side Q_g is maintained to zero. When needed for example in time of grid voltage dip to recover the voltage, the reactive power is needed. On the other hand, the stator side reactive power Q_s is needed to calculate the I_d reference of rotor side current control loop. Here, Q_s is shown in Figure 15. At time 3.15sec I_d is injected as shown in Figure 17, so Q_s is changed with this I_d.
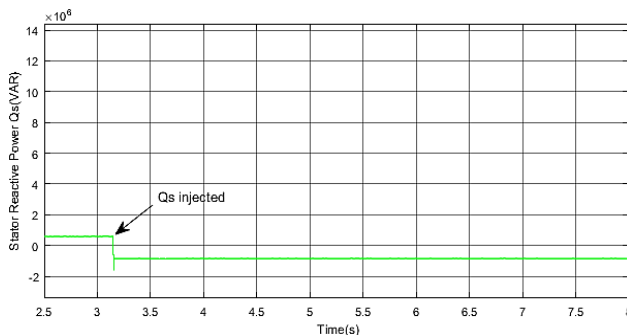
Figure 15: Stator side reactive power Q_s
at a wind speed of 10ms⁻¹
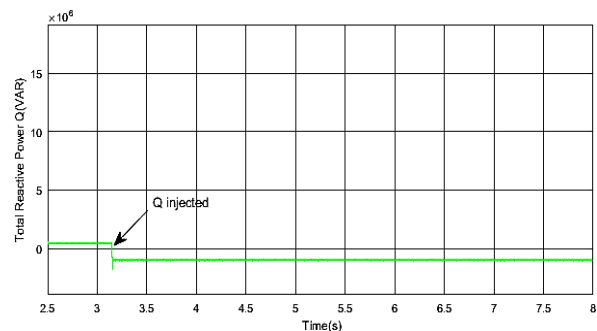
Figure 16: Total reactive power Q at grid
at a wind speed of 10ms⁻¹

Reactive power to be injected to a grid system is defined by the local grid code requirement. Every grid system has a minimum requirement of reactive power that must be supplied by the generator. The total reactive power of the DFIG that is supplied to the grid is shown in Figure 16. It is seen that the reactive power is constant for all time of operation that must be maintained. Direct axis current I_d is shown by the Figure 17. The I_d is set by the stator reactive power Q_s. Here, the I_d is set directly and 1760A is injected at 3.25sec. Hence total reactive power is injected at that moment. A symmetrical fault is intentionally created at the grid at time 3sec and because of this fault the voltage at the grid becomes 10% of the normal operating voltage. When fault occurs there is an excessive amount of rotor current that can damage the converter.
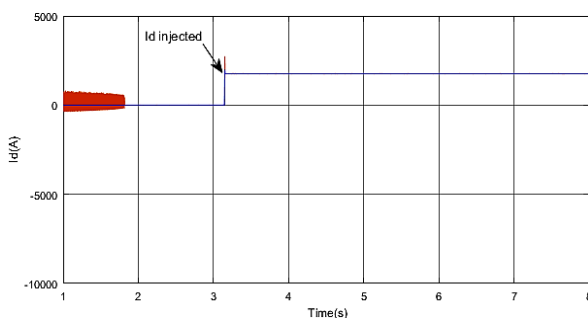
Figure 17: Direct axis current of rotor side I_d
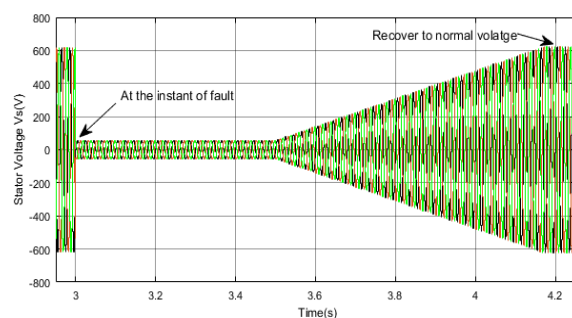
Figure 18: Stator voltage response for a
symmetrical fault at grid.

In order to provide the capability of LVRT capability, the turbine should be connected during the voltage dip so that the crowbar can automatically connect and disconnect itself to the system without removing the DFIG from the grid. Figure 18 shows the voltage waveforms of faulty lines and also shows that the voltage recovering is started at 3.5sec and fully recovered to its normal voltage level at 4.17sec.
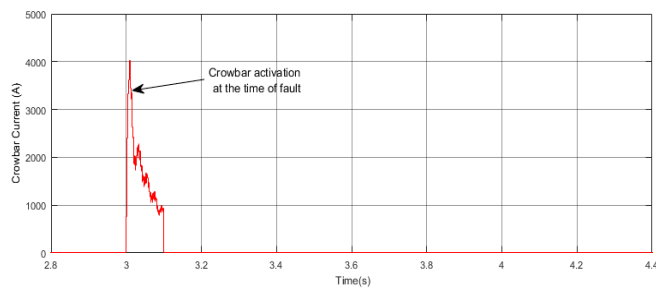
Figure 19: Crowbar activation to recover the fault
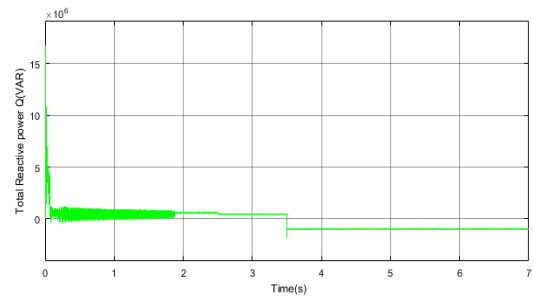
Figure 20: Reactive power injected to
mitigate voltage dip.

When fault occurs the machine losses its control and for LVRT capability of the generator, the crowbar is activated. Figure 19 shows the crowbar activation period which is activated at 3sec when fault is initiated and crowbar is deactivated at 3.1sec when the machine can maintain its control with the existing low voltage. Reactive power Q is injected at 3.5sec to recover the normal voltage level as shown in Figure 20.
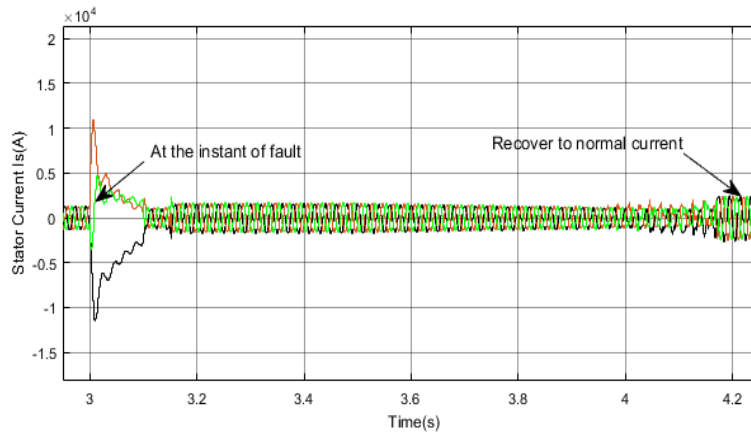

Figure 21: Stator current response for a symmetrical fault at grid

Figure 21 and 22 shows the stator and rotor currents respectively at fault condition whereas Figure 23 shows the stator flux at fault condition. This shows that flux is decreased when crowbar is activated. When flux is recovered to its normal position the currents and voltages come to their normal operating value.
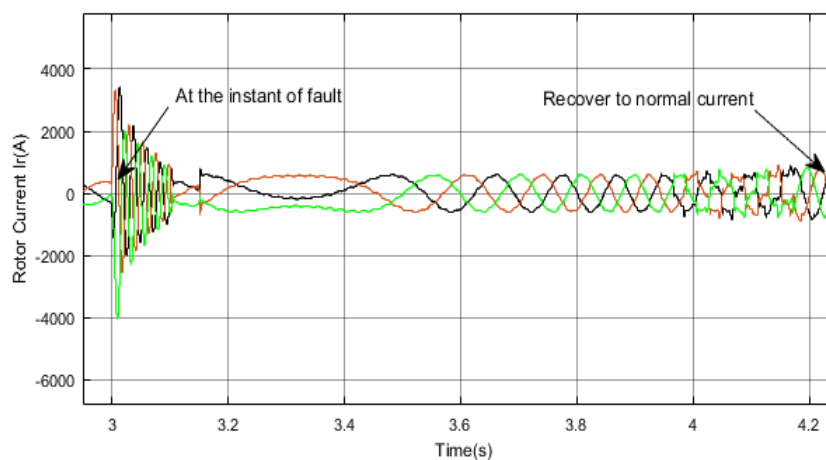

Figure 22: Rotor current response for asymmetrical fault at grid.
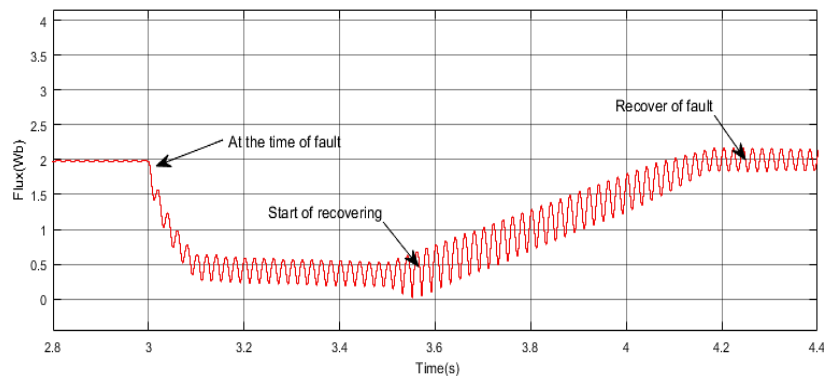
Figure 23: Stator flux response for a symmetrical fault at grid.

VI. CONCLUSION

In this research paper, a doubly fed induction generator is modeled and a vector control strategy of the generator is proposed using PI and PID regulator and machine is model in *d-q* reference frame. For RSC a vector control strategy is proposed with PID current controller and performance is compared with that of PI. For GSC a voltage oriented vector control strategy is proposed and validated in MATLAB Simulink environment. The proposed RSC and GSC can handle about 30% of total power of the machine. The speed response for PID is outperformed PI regulator and reaches its steady value more quickly if PID regulator is used instead of PI, but there is some deviation of actual torque from the reference torque.

The main advantage of using DFIG in wind turbine is that it uses partial power rating of converter where PMSG and SCIG with FPC use the full power converter. An MPPT system is designed for maximum power recovering from wind speed. So, no need to use the speed regulator. An analytical model is developed using state-space representation. The proposed control method for this machine is very reliable and for LVRT of the generator is successfully maintained. A symmetrical fault of 90% voltage dip is intentionally created for 0.5sec. The generator is connected to the grid with the voltage dip without isolation from the grid. The control strategy gains the synchronism of the machine with grid within 0.67sec. This shows the reliability and controllability of the generator.

ACKNOWLEDGEMENT

APPENDIX

Simulation Parameters:

Wind turbine:
Rated power P_n= 2.0 MW
Maximum rotational speed $n_{m\,max}$= 20 rpm
Base wind speed v_B = 10.5 m/s
Rated wind speed v_n = 12 m/s
Rotor radius R = 42 m
C_{pmax}= 0.44
Torque coefficient, λ_{opt}= 7.2
Pitch angle β range 0˚–45˚
Gear ratio n_r/n_m = 100
Inertia J = 127 kg.m^2
Friction coefficient D = 0.01 Nm.s
Air density ρ = 1.225 kg/m^3

DFIG:
Rated stator power P_{ns}= 2 MW
Frequency, f = 50 Hz
Synchronous speed n_s= 1500 rpm (4 poles)
Rated stator voltage V_s= 690 V

Rotor blocked rotor voltage V_r= 2070 V
Stator resistance R_s= 2.6 mΩ
Rotor resistance (referred to stator) R_r = 2.9 mΩ
Stator leakage inductance L_{sl}= 0.087 mH
Rotor leakage inductance L_{r1} (referred to stator) = 0.087mH
Magnetizing inductance L_m= 2.5 mH
DC link capacitance $C_{dc\text{-}link}$=0.08F
Grid side filter resistance R_f=0.00002Ω
Grid side filter inductance L_f=400μH
Crowbar resistance = 0.2 Ω

PI regulator for RSC:
Proportional constant of i_{dr} regulator $K_p\_i_{dr}$= 0.5771
Integral constant of i_{dr} regulator $K_i\_i_{dr}$=491.5995
Proportional constant of i_{qr} regulator $K_p\_i_{qr}$= 0.5771
Integral constant of i_{qr} regulator $K_i\_i_{qr}$= 491.5995

PI regulator for GSC:
Proportional constant of i_{dg} regulator $K_p\_i_{dg}$= 0.004265
Integral constant of i_{dg} regulator $K_i\_i_{dg}$=56.8489
Proportional constant of i_{qg} regulator $K_p\_i_{qg}$= 0.004265
Integral constant of i_{qg} regulator $K_i\_i_{qr}$= 56.8489

PID regulator for RSC:
Proportional constant of i_{dr} regulator $K_p\_i_{dr}$= 0.004265
Integral constant of i_{dr} regulator $K_i\_i_{dr}$=0.085427
Derivative constant of i_{dr} regulator $K_d\_i_{dr}$= 1.59175
Proportional constant of i_{qr} regulator $K_p\_i_{qr}$= 0.004265
Integral constant of i_{qr} regulator $K_i\_i_{qr}$= 0.085427
Derivative constant of i_{qr} regulator $K_d\_i_{qr}$= 1.59175
Filter coefficient N=44.904

REFERENCES

[1] https://wwindea.org/information-2/informatio, accessed March 10, 2019.
[2] J. Rocabert, A. Luna, F. Blaabjerg and P. Rodríguez, "Control of Power Converters in AC Microgrids," in *IEEE Transactions on Power Electronic*s, vol. 27, no. 11, pp. 4734-4749, Nov. 2012.
[3] HuangJiayi, JiangChuanwen, XuRong,"A review on distributed energy resources and MicroGrid,"*Renewable and Sustain Energy Reviews*. 2008, 12, 2472–2483.
[4] Juan M.Lujano-Rojas, Cláudio Monteiro, RodolfoDufo-López, José L.Bernal-Agustín,"Optimum load management strategy for wind/diesel/battery hybrid power systems,"*Renewable Energy* 2012, 44, 288–295.
[5] F. D. Kanellos and N. D. Hatziargyriou, "Control of Variable Speed Wind Turbines in Islanded Mode of Operation," in *IEEE Transactions on Energy Conversion*, vol. 23, no. 2, pp. 535-543, June 2008.
[6] J.E.Paiva, A.S.Carvalho,"Controllable hybrid power system based on renewable energy sources for modern electrical grids," *Renewable Energy* 2013, 53, 271–279.
[7] H. Li and Z. Chen, "Overview of different wind generator systems and their comparisons," in *IET Renewable Power Generation*, vol. 2, no. 2, pp. 123-138, June 2008.
[8] Lie Xu and P. Cartwright, "Direct active and reactive power control of DFIG for wind energy generation," in *IEEE Transactions on Energy Conversion*, vol. 21, no. 3, pp. 750-758, Sept. 2006.
[9] S. Muller, M. Deicke and R. W. De Doncker, "Doubly fed induction generator systems for wind turbines," in *IEEE Industry Applications Magazine*, vol. 8, no. 3, pp. 26-33, May-June 2002.
[10] Petersson, "Analysis, Modeling, and Control of Doubly-Fed Induction Generators for Wind Turbines,"*PhD thesis*, Department of Energy and Environment Chalmers University of Technology, 2003.
[11] Boldea, Variable Speed Generators. CRC Press/Taylor & Francis, 2006.
[12] Erlich, J. Kretschmann, J. Fortmann, S. Mueller-Engelhardt, and H. Wrede, "Modeling of wind turbines based on doubly-fed induction generators for power system stability studies," Vol.22, No.3, August 2007.
[13] R. Cardenas, R. Pena, S. Alepuz and G. Asher, "Overview of Control Systems for the Operation of DFIGs in Wind Energy Applications," in *IEEE Transactions on Industrial Electronics*, vol. 60, no. 7, pp. 2776-2798, July 2013.
[14] Arnaltes, S.; Rodriguez-Amenedo, J.L.; Montilla-DJesus, M.E. Control of Variable Speed Wind Turbines with Doubly Fed Asynchronous Generators for Stand-Alone Applications. *Energies* 2018, *11*, 26.
[15] G. Abad, L. Marroyo, and G. Iwanski, "Doubly Fed Induction Machine: Modeling and Control for Wind Energy Generation, FirstEdition,"*Wiley-IEEE Press*, 2011